

# THE PHOTOSPHERIC TEMPERATURE STRUCTURE OF MAGNETIC FLUXTUBES

S.K. Solanki

*Institute of Astronomy  
ETH Zürich, Switzerland*

## ABSTRACT

The temperature stratifications of plage and network fluxtubes are determined by comparing a large number of observed Fe I and Fe II lines with LTE model calculations. The data are also compared with profiles calculated using different empirical models published in the literature. Thus the sensitivity of the technique employed in the present investigation to changes in the temperature stratification is demonstrated. It is shown that in order to reproduce our data correctly, a sharp dip in the fluxtube temperature must occur in the photosphere, where the temperatures of fluxtube and surroundings become similar (at equal optical depth), contrary to the results of previous models. The effects of different pressure stratifications on the depths of the iron lines are briefly discussed and it is shown that the pressure stratification giving the best agreement with the data corresponds to a rapid expansion of the fluxtube near the height at which the temperature dip occurs.

**Key words:** Fluxtubes—Active regions—Network—Magnetic fields

## 1. INTRODUCTION

A new approach to the empirical modelling of solar magnetic fluxtubes was presented in two recent papers (Solanki and Stenflo, 1984a and b). Using a statistical analysis performed on the parameters of a large number of Fe I and Fe II line profiles, the effects of different physical quantities on these profiles could be partially separated and information gained on the physical structure of fluxtubes.

The two papers mentioned above explored the possibilities of this approach by comparing observed profiles of a large number of lines with the results of a very simple fluxtube model. Thus estimates of the magnetic field strength, magnetic filling factor, microturbulence velocity and the temperature stratification of the fluxtube were made. However, these estimates remain very crude, since they were only meant to illustrate the statistical method of obtaining information on fluxtube properties.

Besides being one dimensional the exploratory model used by Solanki and Stenflo (1984a and b) had two major shortcomings. The temperature difference between the surroundings and the fluxtube at equal optical depth was assumed to vary approximately linearly with optical depth, and the pressure inside the fluxtube was determined by simply shifting the pressure structure of the surroundings down by the Wilson depression. These simple, and probably unrealistic, height dependences for the temperature and the pressure were assumed in order to facilitate the study of the diagnostic power of the statistical method.

One of the aims of this paper is to find more realistic height

dependences for these quantities. We shall concentrate on the temperature, giving only secondary consideration to the pressure and magnetic field, since the field strength can be determined with greater precision using other methods, for example the line ratio technique applied to the complete line profile as illustrated by Stenflo (1984). The pressure can then be calculated directly from the magnetic field if tension forces are neglected.

A second aim is to compare our observations with the profiles resulting from models published in the literature. In this way the results of different modelling techniques can be directly compared with each other.

## 2. METHOD OF DATA REDUCTION

### 2.1. The Data

The observational material used in the present paper has been described in detail by Stenflo et al. (1984). It was obtained with the NSO McMath telescope and the one meter Fourier transform spectrometer adapted to record Stokes  $I$  and  $V$  simultaneously. It consists of high resolution spectra of features near disc centre ranging from the quiet sun network to strong plages, as well as a recording of Stokes  $I$  alone made in a quiet region. This last spectrum has been used to eliminate filling factor effects in the Stokes  $I$  profiles recorded in active regions.

### 2.2. Data Reduction

In order to study the sub-arcsecond fluxtubes, knowledge of the intensity profiles produced completely inside the fluxtube,  $I_V$ , of a number of lines is required. The  $I_V$  profile of a given line can be recovered, in a first order approximation, from its observed Stokes  $V$  profile using the relation

$$\frac{I_c - I_V}{I_c} = -\frac{1}{\Delta\lambda_H} \int_{\lambda_1}^{\lambda} \frac{V(\lambda')}{I_c} d\lambda'. \quad (1)$$

$I_c$  is the intensity of the continuum,  $\lambda$  the wavelength,  $\lambda_1$  the lower integration boundary, and  $\Delta\lambda_H$  the Zeeman splitting given by

$$\Delta\lambda_H = 4.67 \times 10^{-13} g \lambda^2 B, \quad (2)$$

where  $g$  is the Landé factor and must be replaced by the effective Landé factor  $g_{eff}$  for lines with anomalous Zeeman splitting.  $\lambda$ ,  $\lambda_1$ , and  $\Delta\lambda_H$  are in  $\text{\AA}$ , and  $B$  is in G.

Due to the observed area asymmetries,  $A_b$  and  $A_r$ , of the Stokes  $V$  profiles (difference between the areas of the blue and red wings of Stokes  $V$ ) discussed by Solanki and Stenflo (1984a), the continuum has to be renormalized. This is done by multiplying the blue wing of  $V$  by  $\sqrt{A_r/A_b}$  and the red wing of  $V$  by  $\sqrt{A_b/A_r}$  before the integration is carried out.

The reduction procedure has been detailed by Solanki and Stenflo (1984a and b), who have also discussed questions referring to the interpretation of  $I_V$ .

### 2.3. The Chosen Lines and their Parameters

The approximately 450 unblended Fe I and Fe II lines used in the present investigation have been listed by Stenflo and Lindgren (1977), and by Dravins and Larsson (1983) respectively. The parameterisation of the lines follows Solanki and Stenflo (1984a). The only parameters required for our purposes are the line depth ( $d_I$  for Stokes I and  $d_V$  for  $I_V$ ), and the line strength ( $S_I$  and  $S_V$  respectively) defined as the area in Fraunhofer under the half level chord of the line.

## 3. DETERMINATION OF THE TEMPERATURE STRUCTURE

### 3.1 Fluxtube Models and Radiative Transfer

The fluxtube model used in the present paper, though similar to the one described by Solanki and Stenflo (1984a), differs from that model in several important points, and will consequently be described in some detail.

Basically it is a two component model, the non-magnetic part of which is given by the HSRA (Gingerich et al., 1971). The pressure of the magnetic portion can be determined in two ways. a) by specifying a single parameter,  $Z_W$ , which gives the amount by which the pressure structure of the HSRA is shifted down:  $P_{\text{fluxtube}}(Z - Z_W) = P_{\text{HSRA}}(Z)$ , with  $Z$  being the height.  $Z$  increases outwards and  $Z = 0$  at  $\tau_{5000}(\text{HSRA}) = 1$ . b) The pressure at each height is specified directly, allowing different forms of the height variation of the pressure to be tried out.

The temperature stratification is determined by specifying the temperature difference at equal optical depth,  $\Delta T(\tau) = T_{\text{fluxtube}}(\tau) - T_{\text{surroundings}}(\tau)$ , at a number of optical depths and assuming  $\Delta T$  to be approximately linear between them. The number of points,  $N$ , at which  $\Delta T$  is to be specified can be changed. For  $N = 2$  the model used by Solanki and Stenflo (1984a and b) is recovered, while for a larger number of points more general temperature structures are possible.

Once the pressure and temperature have been determined, the density can be derived from the ideal gas equation, and the magnetic field can be calculated using the relation for pressure equilibrium

$$B = \sqrt{8\pi(P_{\text{HSRA}} - P_{\text{fluxtube}})}. \quad (3)$$

A further parameter is the ratio of the microturbulence velocity inside and outside the fluxtube:  $f = \xi_{\text{fluxtube}}/\xi_{\text{HSRA}}$ . The choice of this parameter is irrelevant for the present investigation since the results presented here are derived from the line depths alone.  $f$  has therefore been set to 0.7, a realistic value according to Solanki and Stenflo (1984a).

The LTE radiative transfer calculations are carried out exactly as in Solanki and Stenflo (1984a and b) except that the electron pressure and the continuum opacity are now determined using the code described by B. Gustafsson (1973).

### 3.2. Summary of the Temperature Information Previously Obtained from the Scatterplots

The temperature information obtained by Solanki and Stenflo (1984a and b) was mainly derived from the two scatterplots  $\ln(d_V/d_I)$  vs.  $S_I$  and  $\ln(d_V/d_I)$  vs.  $\chi^*$ , with  $\chi^* = \chi_e + \chi_i$ , where  $\chi_e$  is the excitation potential of the lower level of the line, and  $\chi_i = 0$  eV for Fe I and 7.87 eV, the ionisation potential of neutral iron, for Fe II. They showed how the temperature at two different heights can be determined from these diagrams using their fluxtube model ( $N = 2$ , cf. Sect. 3.1). According to this model  $\Delta T$  increases steeply downwards from a value of 0–300 K at  $\tau_{5000} = 10^{-4}$  to 1000 K at  $\tau_{5000} = 1$  for network fluxtubes, but reaches only 300–400 K at  $\tau_{5000} = 1$  for plage fluxtubes. It was also pointed out that by comparing how a model fitted both the plots ( $\ln(d_V/d_I)$  vs.  $S_I$  and vs.  $\chi^*$ ) simultaneously, it would be possible to set some constraints on the height dependence of the temperature. For the network at least, this comparison suggested that a linear  $\Delta T(\tau)$  was not the ideal choice.

It was also found that these two plots are independent of the Wilson depression, i.e. of the assumed magnetic field strength, as

long as the pressure inside the fluxtube is determined by method a) (cf. Sect. 3.1). The effects of other  $T$  and  $B$  stratifications on these plots were not studied.

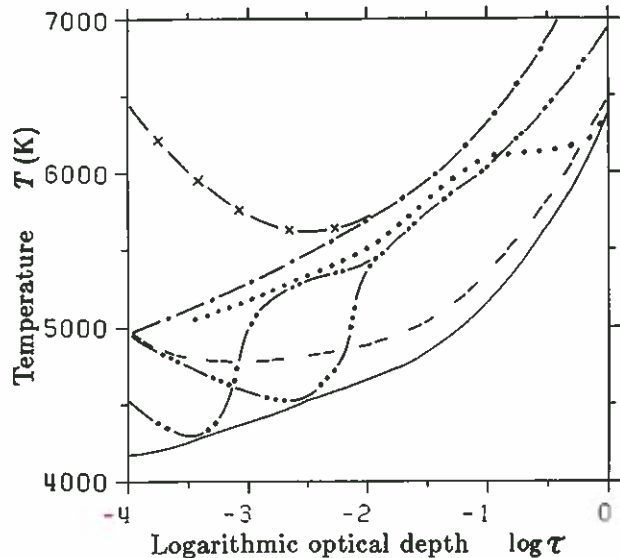


Fig. 1a. Temperature stratifications of different network models relative to the HSRA (solid line). ---: Stenflo (1975); .....: Hirayama (1978) model B; —x—: Koutchmy and Stellmacher (1978); —•—: Stellmacher and Wiehr (1979); —□—: model 3E; —△—: model 6N.

### 3.3. The Temperature with Fixed Pressure Stratification

In order to determine the temperature stratification about 100 models have been evaluated, all being identical in every respect but their temperatures. For each model the profiles of about 40 hypothetical Fe I and Fe II lines having different oscillator strengths and excitation potentials have been calculated.

One of the first results to emerge from these calculations was that in practically all models the Fe I and Fe II line cores (it should be kept in mind that only the line depths are evaluated here) are sensitive to the temperature over two different height ranges, the strongest Fe II lines being formed close to the level where the weakest Fe I lines are formed. This result that the Fe I lines are formed higher in the atmosphere seems to contradict the sensitivity of the weaker Fe I lines to the temperature at  $\tau_{5000} = 1$  found by Solanki and Stenflo (1984a). However, this

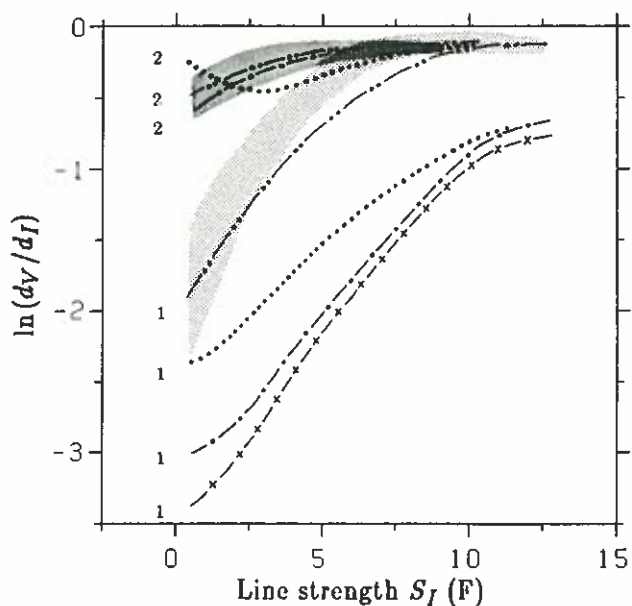


Fig. 1b.  $\ln(d_V/d_I)$  vs.  $S_I$  for network data (Fe I: light shading, Fe II: dark shading), and the models: .....: Hirayama (1978) model B; —x—: Koutchmy and Stellmacher (1978); —•—: Stellmacher and Wiehr (1979); —□—: models 3E and 6N. Model curves labeled '1' refer to Fe I, those labeled '2' refer to Fe II.

sensitivity was a result of the coupling between the temperatures at different heights due to the assumed linearity of  $\Delta T(r)$  in their exploratory model.

Another interesting result is that the best fit temperature stratification is not unique, with different models giving similar fits to the data. Two such models which give good fits to our network data (models 3E and 6N) are plotted in Fig. 1a, together with the common network and plage model of Stenflo (1975), Hirayama's network model B (1978), the filigree model of Koutchmy and Stellmacher (1978), the common filigree and faculae model of Stellmacher and Wiehr (1979), and the HSRA.

How these models compare with the data is illustrated in Fig. 1b, where  $\ln(d_V/d_I)$  is plotted vs.  $S_I$  for the data (light shading: Fe I lines, dark shading: Fe II lines), and for lines calculated using some of the models plotted in Fig. 1a. The symbols used for each model are the same in both plots. In order to keep Fig. 1b from getting too crowded the Fe II curve of Koutchmy and Stellmacher (1978) which is very similar to the curve resulting from the Stellmacher and Wiehr (1979) model together with the curves of Stenflo's (1975) model have not been plotted. However the results of Stenflo's model can be seen in Fig. 2b. The results of the models 3E and 6N lie so close together that they are both represented by the same curves.

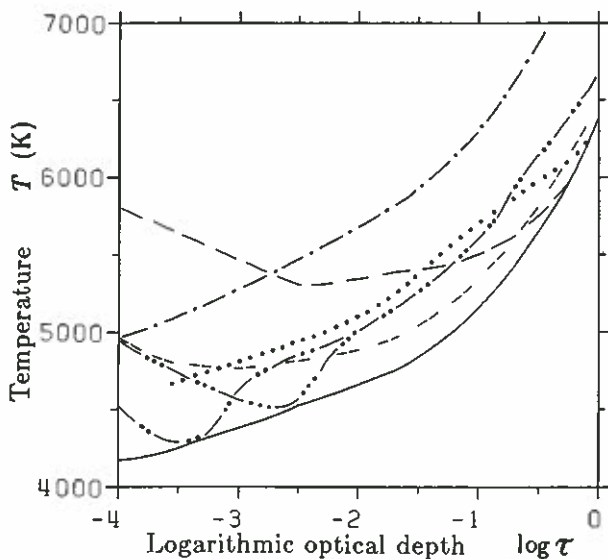


Fig. 2a. Temperature stratifications of different plage models relative to the HSRA (solid line). --- Stenflo (1975); ..... Hirayama (1978) model Z; -.-.- Chapman (1979); - - - - - Stellmacher and Wiehr (1979); - - - - - model 6K; - - - - - model 6P.

Fig. 2a shows  $T(r)$  for the HSRA, Stenflo's (1975) model, model Z of Hirayama (1978), the facular model of Chapman (1979), the model of Stellmacher and Wiehr (1979) and two of our plage models giving good fits to the data (6K and 6P). The plage data are compared with the results of the model calculations in Fig. 2b. To avoid crowding, the results of the model of Stellmacher and Wiehr (1979) have not been repeated from Fig. 1b.

Finally, it is shown in Fig. 3 how the different models compare with the data in the  $\ln(d_V/d_I)$  vs.  $\chi^*$  diagram using data from a network region and the models of Stenflo (1975), Hirayama (1978, model B), Koutchmy and Stellmacher (1978), Chapman (1979), Stellmacher and Wiehr (1979), and our network models 3E and 6N. These two models give such similar results that again only one curve has been plotted. The models have been shifted in such a way that they all reproduce the Fe II data.

In the following we list some comments on the figures and the models presented above:

- The large spread of the model curves in Figs. 1b and 2b is evidence for the temperature sensitivity of our method. It also reflects the different types of data on which the models are based. Usually the data come from more or less high spatial resolution Stokes I or continuum observations (and sometimes both), the exceptions being Stenflo (1975), who also used the Stokes V profiles of two lines, and our models, which are based on the Stokes I and V profiles of hundreds

of lines. The models using Stokes I and V represent just the magnetic regions of the solar photosphere, whereas other models may reproduce properties of non-magnetic regions as well. One component 'average facula' models (e.g. Shine and Linsky, 1974) have not been included, since they represent averages of the magnetic and non-magnetic components of active regions and thus cannot be directly compared to our models.

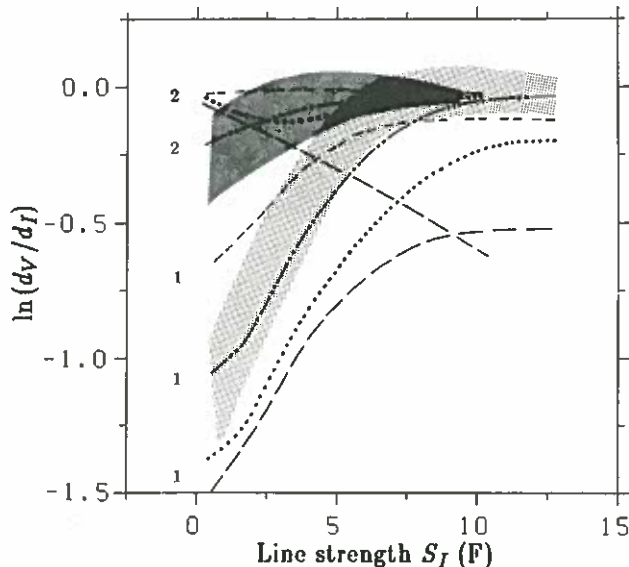


Fig. 2b.  $\ln(d_V/d_I)$  vs.  $S_I$  for plage data (Fe I: light shading, Fe II: dark shading), and the models: --- Stenflo (1975); ..... Hirayama (1978) model Z; -.-.- Chapman (1979); - - - - - models 6K and 6P. Model curves labeled '1' refer to Fe I, those labeled '2' refer to Fe II.

- It is confirmed that network and plage fluxtubes have a different temperature structure, with network fluxtubes having higher temperatures in their lower regions, as pointed out by Solanki and Stenflo (1984a), and by Hirayama (1978). However Hirayama used the expression facular granules and rejected the idea of the magnetic field outside sunspots being concentrated into small fluxtubes.

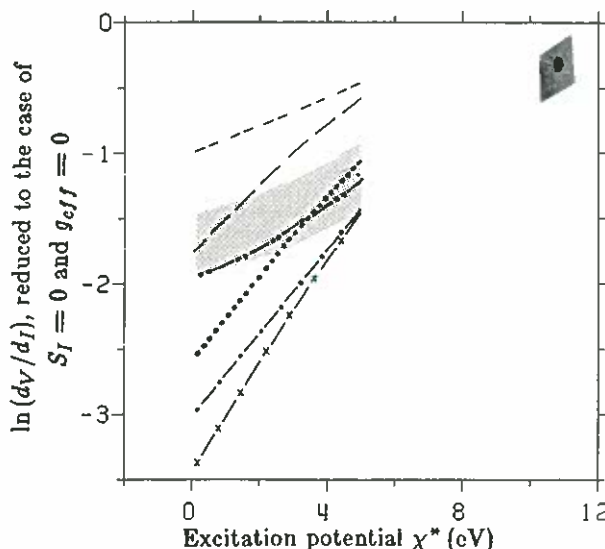


Fig. 3.  $\ln(d_V/d_I)$  vs.  $\chi^*$  for network data (Fe I: light shading, Fe II: dark shading) and the models: --- Stenflo (1975); ..... Hirayama (1978) model B; -x-x- Koutchmy and Stellmacher (1978); - - - - - Stellmacher and Wiehr (1979); - - - - - models 3E and 6N.

- Although the temperature structures of models 3E and 6N may look very different at first sight, they have certain important features in common. The main difference is the temperature at  $\tau_{5000} = 10^{-4}$ . Whereas model 3E has  $\Delta T(r = 10^{-4}) = 400$  (compatible with the UV observations of Cook

et al. (1983)), model 6N is similar to Stenflo's (1975) model in the upper photosphere. The Fe I lines are formed around and immediately below the temperature minimum of the respective model atmosphere. Thus the higher temperature of model 6N at  $\tau = 10^{-4}$  leads the Fe I lines to be formed further down, so that we "see" different heights when we look at the Fe I lines in the two models. The structure of the models below their respective temperature minima is very similar, so that model 6N is very similar to model 3E with the temperature minimum shifted down by a factor of ten in the optical depth. The same comment is valid for the network models 6K and 6P. The important point is that the approximate shape of the temperature stratification remains the same. In particular a pronounced depression in  $T$  is needed at some height, where the fluxtube temperature approaches the temperature of the surroundings at equal optical depth. Whether this minimum in the temperature is real or is an artifact of the simplified model assumptions made in Section 3.1 cannot be decided at present.

- All the models except Chapman's reproduce the Fe II lines fairly well. This reflects the relative temperature insensitivity of Fe II.
- The fit to our data by our models, though reasonable is not perfect. In particular the calculated depths of the Fe I lines with line strengths between 4 and 8 Fraunhofer are smaller than the observed values in both plage and network. The difference is particularly noticeable in the network. A number of explanations for this discrepancy suggest themselves. The simplest is that we just have not found the correct temperature stratification yet. Other possibilities include effects resulting from departures from LTE, from the fluxtube geometry, from the observed asymmetries of the Stokes  $V$  profiles, from the chosen pressure structure, or from a combination of some or all of these. Whereas the quantitative determination of any one of the first three effects is a sizable task by itself and lies well beyond the scope of the present paper, the last effect can be studied fairly easily and is the subject of the following section.

#### 3.4. Influence of the Pressure Stratification

Using models having the same temperature structure but different pressure stratifications, the influence of pressure on the spectrum has been analysed in a crude way. It is found that a proper choice of the pressure stratification can improve the agreement between our models and the data in Fig. 2b almost to perfection. However, this effect on the spectrum is critically dependent on the shape of the pressure curve and on the relative pressure and temperature stratifications. When translated into a magnetic field strength using eq. (3), the most successful pressure stratification gives a steep drop in the magnetic field at about the same height at which the temperature drops too. A similar magnetic field structure also improves the fit of our plage models to the data considerably. The main difference between the plage and network magnetic field stratifications is that in the network the magnetic field drops to a lower value than in the plage.

It is of interest to note that the pressure stratifications which produce these improvements are very similar to the ones that best reproduce the Stokes  $V$  asymmetries in unpublished calculations by the author. The obvious interpretation would be a fanning out of the magnetic field at this height. Further up the magnetic field again assumes a more gentle gradient, which could be a result of neighbouring fluxtubes coming into contact with each other due to their rapid expansion. In this picture the plage fluxtubes cannot expand as much as the network fluxtubes due to the larger magnetic filling factors in the plages, in agreement with our result that the magnetic field decreases to a lower value in the network. However, we would like to caution that these results are only based on a very brief analysis and that more thorough investigations are needed.

#### 4. CONCLUSIONS

We have utilized the technique described by Solanki and Stenflo (1984a and b) to determine the temperature structures of plage and network fluxtubes. The results of our model, which shows the temperature to have a pronounced depression at the height of formation of the Fe I spectrum, have been compared with

those of other empirical models. As may be expected for models based on quite different data, the resulting line profiles vary considerably. Since our model is based on Stokes  $V$  data it has the advantage that it should be free from the problems caused by straylight from non-magnetic regions, which have plagued most empirical models in the past.

The interpretation of the temperature dip in our model is left open. We limit ourselves to remarking that the results of models with different pressure stratifications indicate a rapid expansion of the fluxtubes. The need for more general two dimensional fluxtube models than those based on the similarity assumption (Schlüter and Temesváry, 1958; Osherovich et al., 1983) is clearly felt. Giovanelli (1980) has presented empirical evidence indicating very rapid expansion around and above the temperature minimum leading to canopies, which however spread over areas larger than those covered by our observations, and probably represent a different (though related) phenomenon as compared with the expansion discussed in Section 3.4.

Another open question is the fluxtube temperature structure above the level at which most of the Fe I lines are formed. This level is at about  $\log \tau = -2$  in the models 6N and 6P, and could lie even lower in the photosphere. This temperature can best be determined by carrying out NLTE calculations. Even the present work is probably affected by departures from LTE, since we have three Fe I lines in our sample stronger than Fe I 5434 Å, the core of which is formed in NLTE in the quiet sun atmosphere (Altrock et al., 1975). The higher layers can however be reached by the moderately strong Fe I lines if their centre-to-limb variations are used.

#### ACKNOWLEDGEMENTS

The author wishes to thank J.O. Stenflo for his guidance and for the many fruitful discussions. The continuum opacity code was provided by Å. Nordlund, which is gratefully acknowledged.

#### REFERENCES

- Altrock, R.C., November, L.J., Simon, G.W., Milkey, R.W., Worden, S.P.: 1975, *Solar Phys.* **43**, 33.  
 Chapman, G.A.: 1979, *Astrophys. J.* **232**, 923.  
 Cook, J.W., Brueckner, G.E., Bartoe, J.-D.F.: 1983, *Astrophys. J.*, **270**, L89.  
 Dravins, D., Larsson, B.: 1984, in S.L. Keil (ed.), *Small-Scale Dynamical Processes in Quiet Stellar Atmospheres*, National Solar Observatory, in press.  
 Osherovich, V.A., Flå, T., Chapman, G.A.: 1983, *Astrophys. J.* **286**, 412.  
 Gingerich, O., Noyes, R.W., Kalkofen, W., Cuny, Y.: 1971, *Solar Phys.* **18**, 347.  
 Giovanelli, R.G.: 1980, *Solar Phys.* **68**, 49.  
 Gustafsson, B.: 1973, *Uppsala Astron. Obs. Ann.*, **5**, No. 6.  
 Hirayama, T.: 1978, *Publ. Astron. Soc. Japan* **30**, 337.  
 Koutchmy, S., Stellmacher, G.: 1978, *Astron. Astrophys.* **67**, 93.  
 Schlüter, A., Temesváry, S.: 1958, in 'Electromagnetic Phenomena in Cosmical Physics', *IAU Symp.* **6**, 263.  
 Shine, R.A., Linsky, J.L.: 1974, *Solar Phys.* **37**, 145.  
 Solanki, S.K., Stenflo, J.O.: 1984a, *Astron. Astrophys.*, in press  
 Solanki, S.K., Stenflo, J.O.: 1984b, *Astron. Astrophys.*, submitted  
 Stellmacher, G., Wiehr, E.: 1979, *Astron. Astrophys.* **75**, 263.  
 Stenflo, J.O.: 1975, *Solar Phys.* **42**, 79.  
 Stenflo, J.O.: 1984, in *Adv. Space Research*, Proc. COSPAR meeting in Graz, Pergamon Press, in press.  
 Stenflo, J.O., Lindegren, L.: 1977, *Astron. Astrophys.* **59**, 367.  
 Stenflo, J.O., Harvey, J.W., Brault, J.W., Solanki, S.K.: 1984, *Astron. Astrophys.* **131**, 333.